Split explicit methods

Almut Gassmann

Meteorological Institute
of the University of Bonn

Germany

Two common methods

applied to nonhydrostatic compressible equations

Semi-Implicit/ Semi-Lagrange		Split-Explicit
completely implicit	fast waves	horizontally explicit vertically implicit
Poisson equation	time stepping	fractional steps
Lagrangian	advection	Eulerian
large time steps possible	advantages	straightforward numerics do well on parallel platforms
terrain-following coords choice of basic state	difficulties	numerical stability proper splitting of terms

Split explicit methods

1) How to divide the terms into slow and fast ones?

2) How to couple slow and fast processes tightly?

3) How to ensure numerical stability?

4) How to define the advection algorithm?

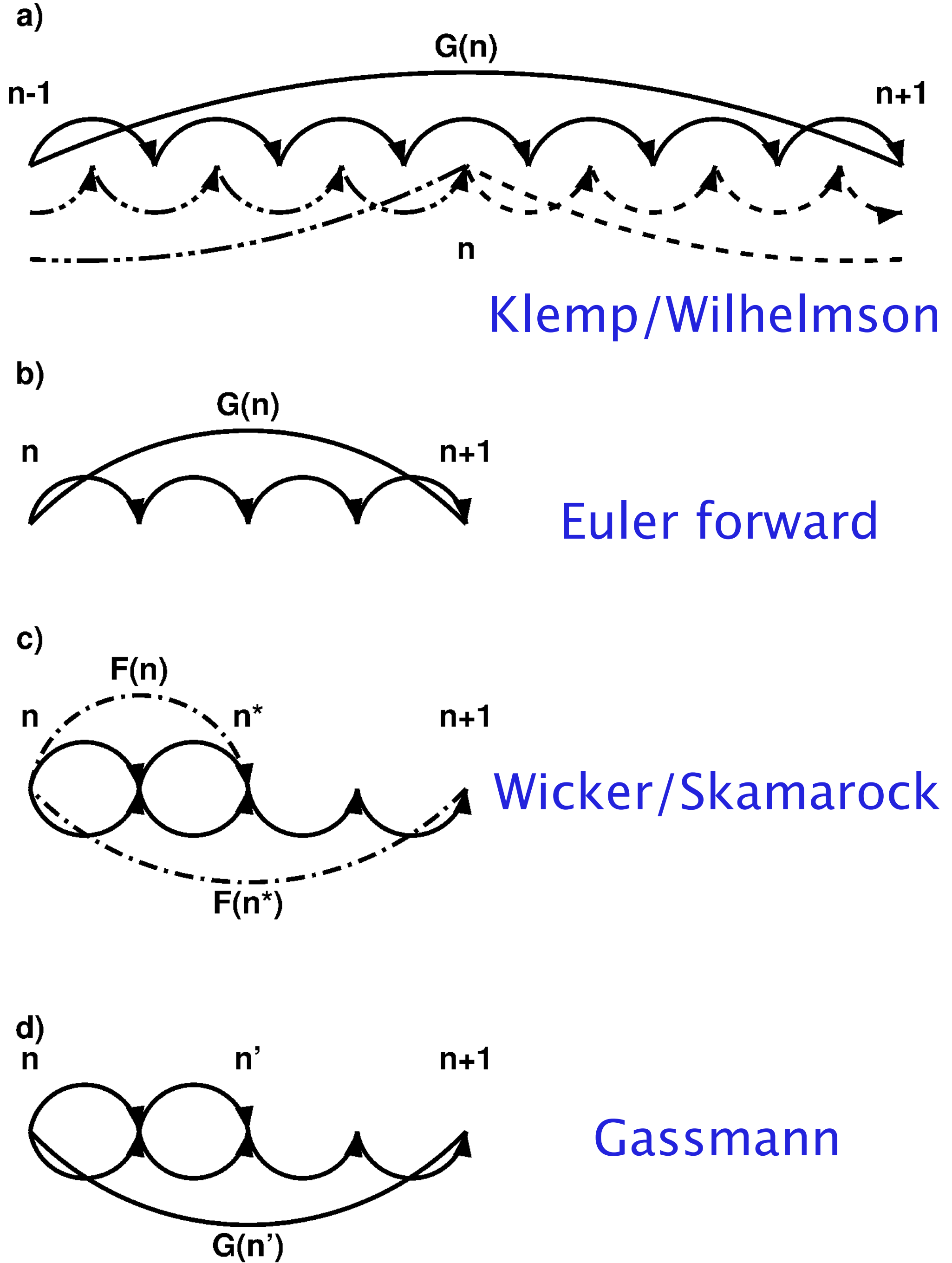

Divide equations into slow and fast parts – Investigate fast modes

Linear wave analysis of...

$$\frac{\partial \hat{u}}{\partial t} + \frac{\partial \hat{p}}{\partial x} = 0$$

$$\frac{\partial \hat{w}}{\partial t} + \left(\frac{\partial}{\partial z} - \frac{1}{2H} + \frac{g}{R\bar{T}}\right)\hat{p} - \frac{g}{c_p\bar{T}}\hat{T} = 0$$

$$\frac{\partial \hat{p}}{\partial t} - g\hat{w} + c_s^2\left(\frac{\partial \hat{u}}{\partial x} + \left(\frac{\partial}{\partial z} + \frac{1}{2H}\right)\hat{w}\right) = 0$$

$$\frac{\partial \hat{T}}{\partial t} - \mu g\left(1 - \frac{N^2}{N_0^2}\right)\hat{w} + c_s^2\left(\frac{\partial \hat{u}}{\partial x} + \left(\frac{\partial}{\partial z} + \frac{1}{2H}\right)\hat{w}\right) = 0$$

...gives us the dispersion relation for acoustic and gravity waves...

$$\frac{1}{c_s^2}\omega^4 - \omega^2\left(k^2 + m^2 + \frac{1}{4H^2}\right) + k^2N^2 = 0$$

$$\omega_a^2 \approx c_s^2\left(k^2 + m^2 + \frac{1}{4H^2}\right)$$

...wherein these both modes are coupled via the divergence.

$$\omega_g^2 \approx \frac{k^2N^2}{k^2 + m^2 + \frac{1}{4H^2}} .$$

As a consequence the acoustic and gravity modes are not strictly separable. But this was ignored in the past by the pioneers in this working field.

Divide equations into slow and fast parts – Investigate fast modes

Numerical stability analysis of (LM-equations) ...

$$\frac{u^{\nu+1}-u^{\nu}}{\Delta\tau} = -\frac{\partial p^{\nu}}{\partial x} + \alpha_h \Delta\tau c_s^2 \frac{\partial D^{\nu}}{\partial x}$$

$$\frac{w^{\nu+1}-w^{\nu}}{\Delta\tau} = -\left(\frac{\partial}{\partial z} - \frac{1}{2H}\right)\left(\beta^+ p^{\nu+1} + \beta^- p^{\nu}\right) - \frac{g}{R\bar{T}}\left(\beta^+ p^{\nu+1} + \beta^- p^{\nu}\right) + \frac{g}{c_p \bar{T}}\left(\beta^+_{lm} T^{\nu+1} + \beta^-_{lm} T^{\nu}\right) + \alpha_v \Delta\tau c_s^2 \left(\frac{\partial}{\partial z} + \frac{1}{2H}\right)\left(\beta^+ D^{\nu+1} + \beta^- D^{\nu}\right)$$

$$\frac{T^{\nu+1}-T^{\nu}}{\Delta\tau} = -c_s^2\left(\frac{\partial}{\partial z} + \frac{1}{2H}\right)\left(\beta^+ w^{\nu+1} + \beta^- w^{\nu}\right) - c_s^2 \frac{\partial u^{\nu+1}}{\partial x} + \mu\, g\left(1 - \frac{N^2}{N_0^2}\right)\left(\beta^+ w^{\nu+1} + \beta^- w^{\nu}\right)$$

$$\frac{p^{\nu+1}-p^{\nu}}{\Delta\tau} = \left(g - c_s^2\left(\frac{\partial}{\partial z} + \frac{1}{2H}\right)\right)\left(\beta^+ w^{\nu+1} + \beta^- w^{\nu}\right) - c_s^2 \frac{\partial u^{\nu+1}}{\partial x}$$

terms for divergence damping

critical points concerning LM / MM5

Divide equations into slow and fast parts – Investigate fast modes

...yields a matrix equation like $$\mathbf{B}\Phi^{\nu+1} = \mathbf{C}\Phi^{\nu}$$

...and an amplification matrix $$\mathbf{A} = \mathbf{B}^{-1}\mathbf{C}$$

...whose eigenvalues must not exceed 1 for numerical stability.

But...
If the temperature part of the buoyancy term are treated explicitly for an isothermal atmosphere, the gravity waves become unstable!

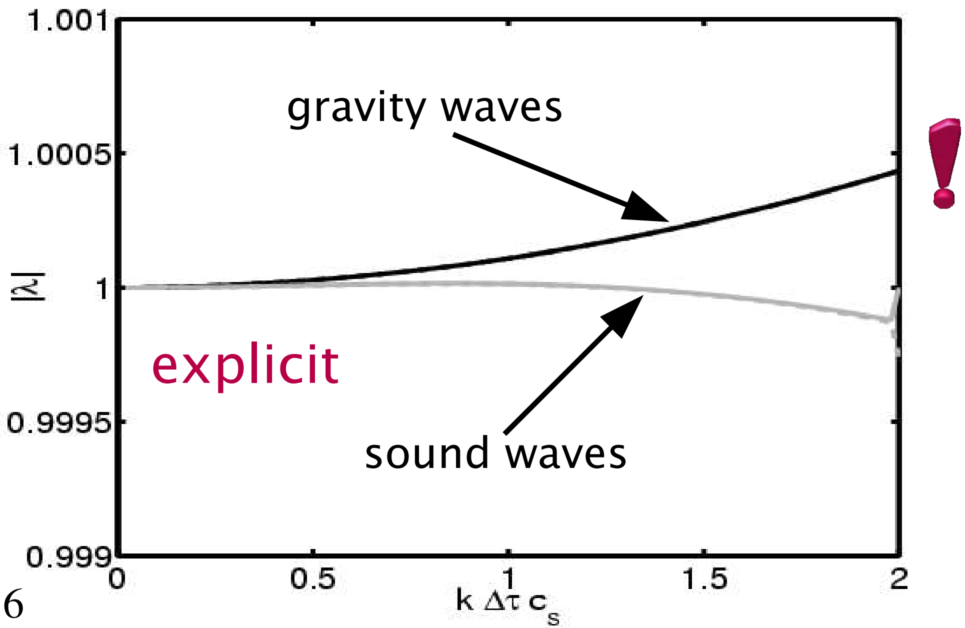

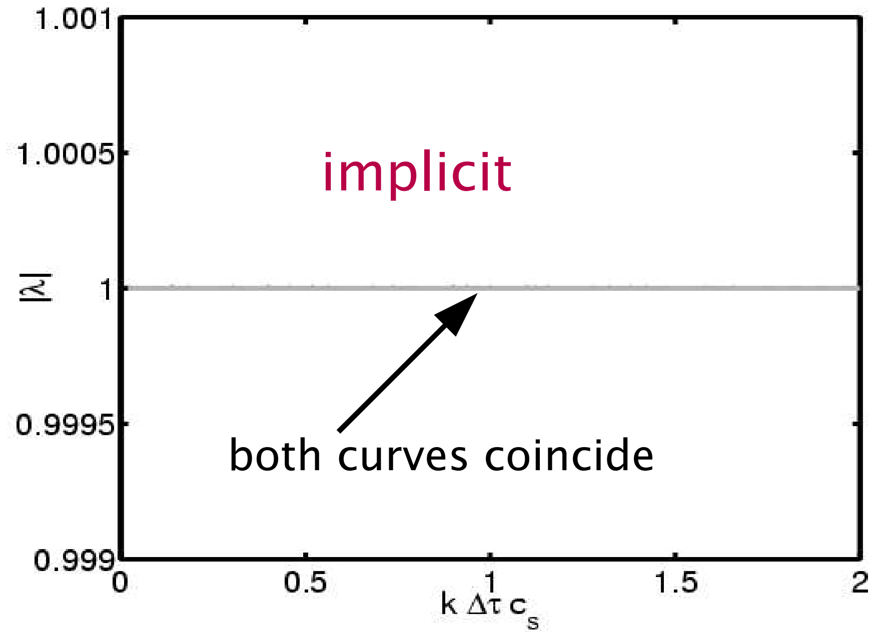

Divide equations into slow and fast parts - Investigate fast modes

For the correct representation of the actual stability (N^2), the vertical advection of pressure and temperature is required in the fast waves part.

$N^2=0.0001/s^2$

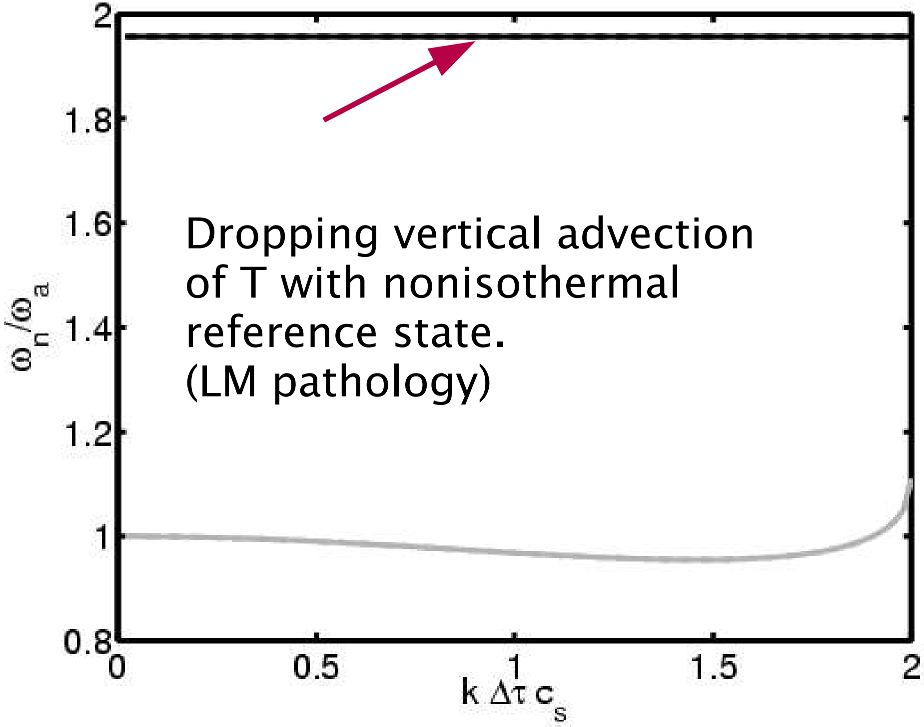

$N^2=0.0001/s^2$

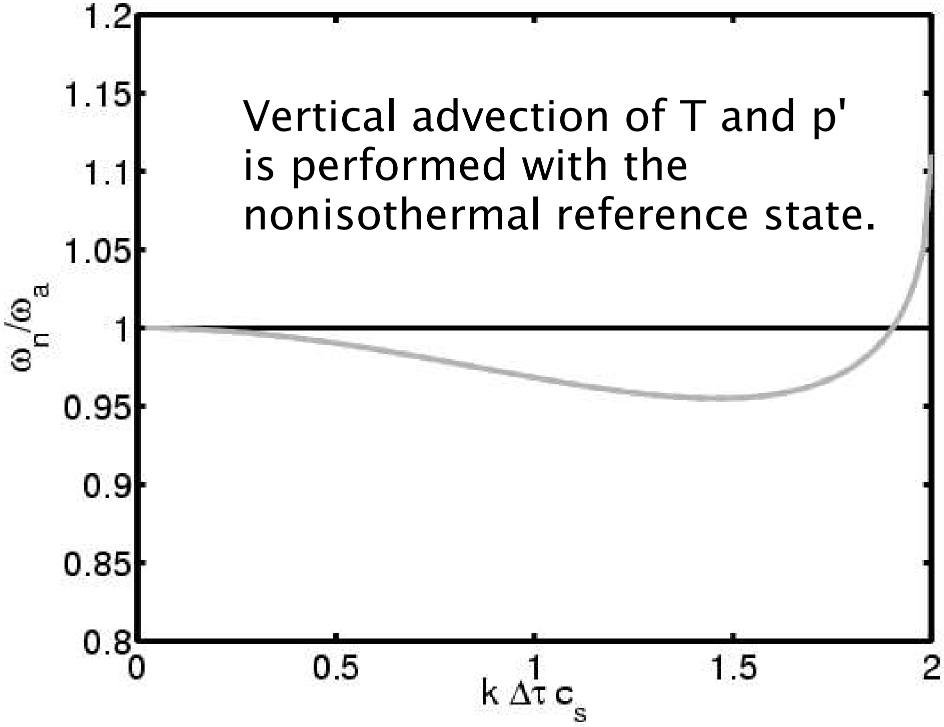

Divide equations into slow and fast parts - Investigate fast modes

As we shall see, some damping of sound waves is required in the splitting scheme...

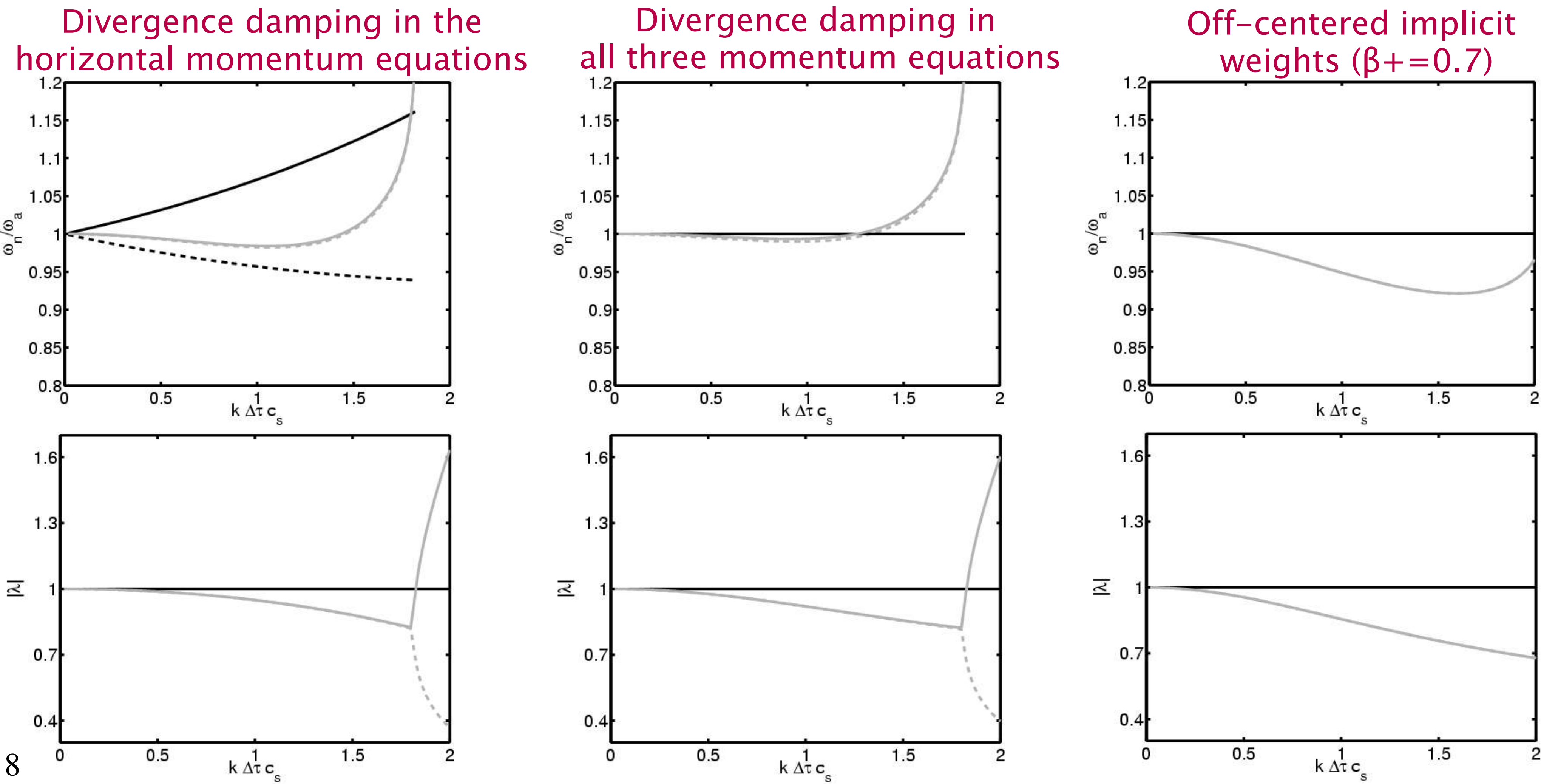

Divide equations into slow and fast parts – Investigate fast modes

Divergence damping analysis

Isotropic divergence damping

$$\frac{1}{c_s^2}\omega^4 + i\gamma\left(k^2 - \left(im + \frac{1}{2H}\right)^2\right)\frac{\omega^3}{c_s^2} - \kappa^2\omega^2 + k^2N^2 = 0$$

damping coefficient

$$\omega_s^{+,-} \approx \pm\kappa c_s\left(1 - \frac{\gamma^2\kappa^2}{4c_s^2}\right)^{1/2} - i\frac{1}{2}\gamma\kappa^2$$

$$\omega_g^{+,-} \approx \pm\frac{kN}{\kappa}.$$

Sound waves are damped.
Gravity waves remain unmodified.

Horizontal divergence damping

$$\frac{1}{c_s^2}\omega^4 + i\gamma_h k^2\frac{\omega^3}{c_s^2} - \kappa^2\omega^2 - i\gamma_h k^2\left(im + \frac{1}{2H}\right)\frac{g}{c_s^2}\omega + k^2N^2 = 0$$

$$\omega_s^{+,-} \approx \pm\kappa c_s\left(1 - \frac{\gamma_h^2 k^4}{4c_s^2\kappa^2}\right)^{1/2} - i\frac{1}{2}\gamma_h k^2$$

Sound waves are damped proportionally to the horizontal wave number.

$$\omega_g^{+,-} \approx \pm\frac{kN}{\kappa}\left(1 + \frac{1}{4}\gamma_h^2\frac{\kappa^2}{k^2N^2}\left(\frac{g}{c_s^2}\frac{k^2m}{\kappa^2}\right)^2\right)^{1/2} + \frac{1}{2}\gamma_h\frac{g}{c_s^2}\frac{k^2m}{\kappa^2}$$

Gravity waves are altered in phase and become faster or slower.

Conclusions from this section

- Numerical stability is required for fast waves part alone.
- A horizontally forward-backward explicit and vertically implicit numerical scheme is applied.
- Acoustic and gravity modes are coupled via the divergence and, therefore, are not separable.
- All terms relevant for vertical structure and wave propagation must be treated within the fast waves part and with the same implicity weights.
- Divergence damping should only be used if it is applied to all three momentum equations. Off-centering the implicity weights is an altenative damping mechanism.

Numerical analysis of the sound advection system

$$\frac{\partial u}{\partial t} + c_s \frac{\partial \hat{p}}{\partial x} = -U \frac{\partial u}{\partial x}$$

$$\frac{\partial \hat{p}}{\partial t} + c_s \frac{\partial u}{\partial x} = -U \frac{\partial \hat{p}}{\partial x}$$

fast modes
sound waves

slow modes
advection terms

For comparison of different schemes we must define a common advection scheme: Runge–Kutta 2nd order in time and 3rd order in space.

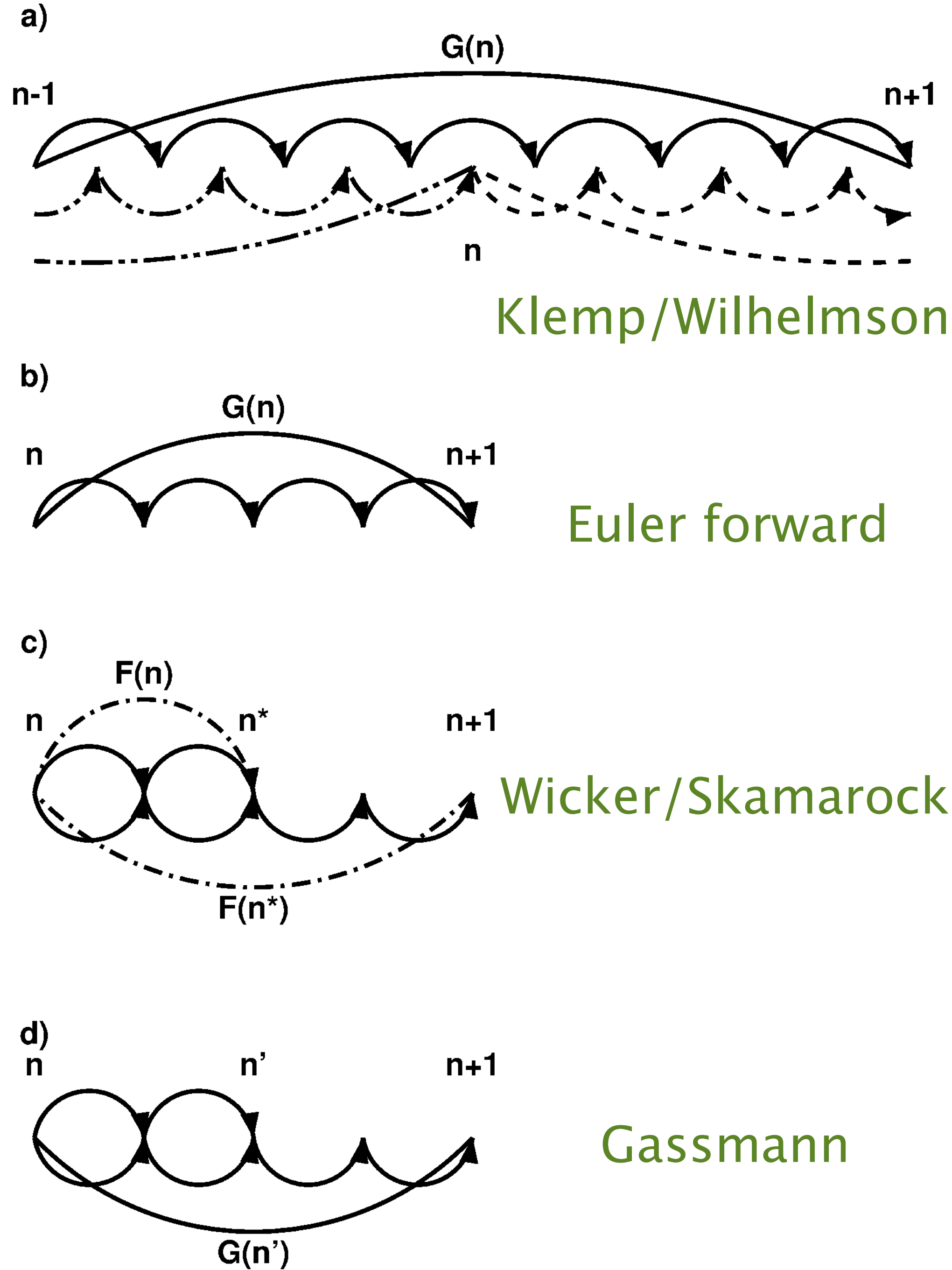

Numerical analysis of the sound advection system

Example: Euler scheme

$$u_{i+1/2}^{m+1} = u_{i+1/2}^{m} - \Delta\tau c_s \frac{\hat{p}_{i+1}^{m} - \hat{p}_{i}^{m}}{\Delta x} + \Delta\tau G(u)_{i+1/2}^{n}$$

$$\hat{p}_{i}^{m+1} = \hat{p}_{i}^{m} - \Delta\tau c_s \frac{u_{i+1/2}^{m+1} - u_{i-1/2}^{m+1}}{\Delta x} + \Delta\tau G(\hat{p})_{i}^{n}$$

RK2-Advection

(Runge-Kutta 2nd order in time)

$$\psi_i^{n^*} = \psi_i^n + \frac{\Delta t}{2} F(\psi^n)_i$$

$$\psi_i^{n+1} = \psi_i^n + \Delta t F(\psi^{n^*})_i$$

$$G(\psi)_i^n = \frac{\psi_i^{n+1} - \psi_i^n}{\Delta t} = F(\psi^{n^*})_i = F(\psi^n + \frac{\Delta t}{2} F(\psi^n))_i$$

3rd order in space (for U>0)

$$F(\psi)_i = -\frac{U}{6\Delta x}\left(\psi_{i-2} - 6\psi_{i-1} + 3\psi_i + 2\psi_{i+1}\right)$$

Fourier representation in space

$$\tilde{k}_U = \frac{1}{3}(\sin(k\Delta x)(4 - \cos(k\Delta x)) - i(\cos(k\Delta x) - 1)^2).$$

dimensionless wavenumber

$$\mathcal{G} = -i\tilde{U}\tilde{k}_U - \frac{1}{2}\tilde{U}^2\tilde{k}_U^2 + \mathcal{O}(\Delta t^3)$$

Courant number for advection

Imaginary part is negative and leads to damping

Numerical analysis of the sound advection system

The computations are performed on a staggered C-grid with forward–backward differencing for the fast waves part and the commonly defined advection algorithm.

Number of small time steps per large step: N=4
u=0.75,cs=3,dx=dt=1 are nondimensional numbers

Euler forward

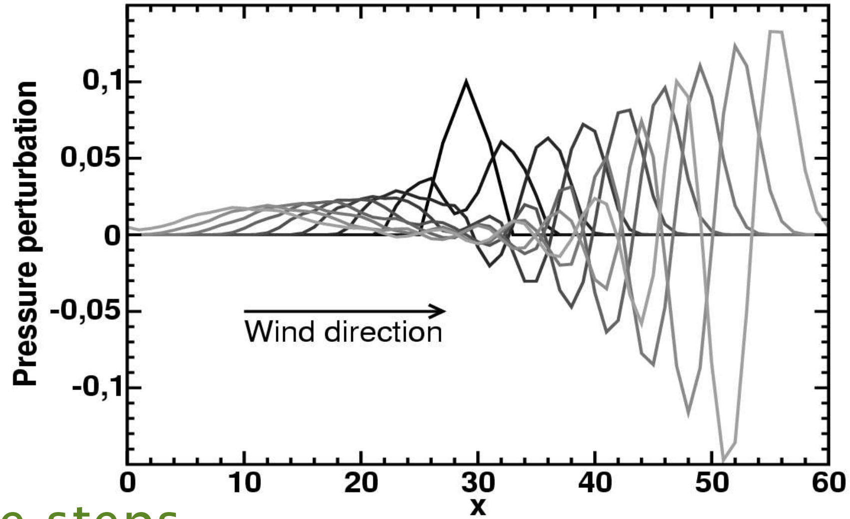

First 8 time steps

Wicker/Skamarock

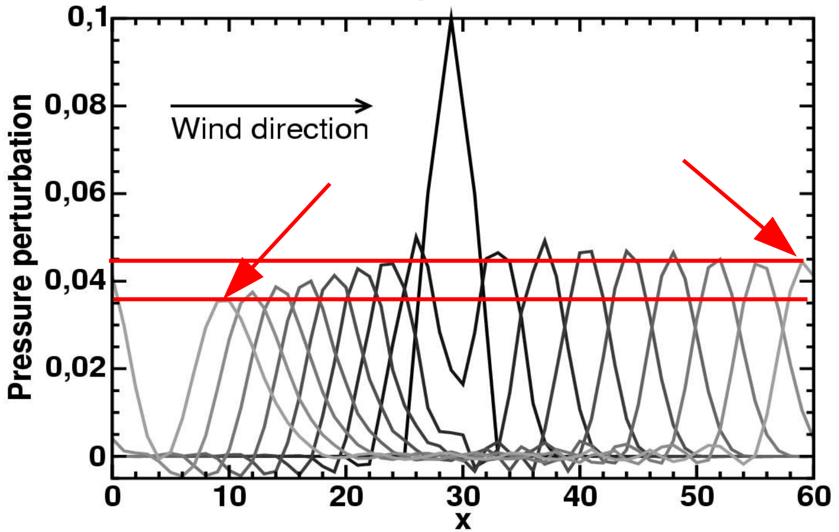

Gassmann

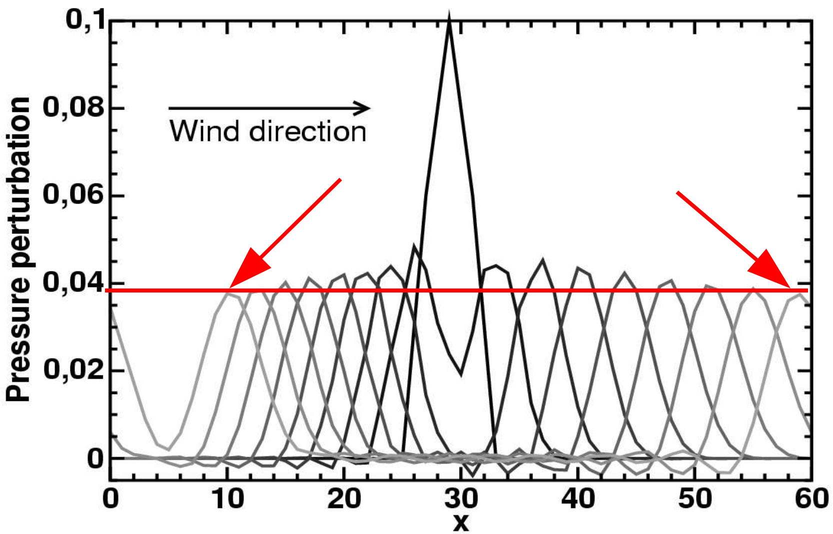

Numerical analysis of the sound advection system

Expansion of the squared eigenvalues of the amplification matrix:

$$|\lambda_{1,2}|^2 = 1 + 2\Im(k_U)U + 2\Im(k_U)^2 U^2 \pm S.E.T. + H.O.T.$$

wavenumber for the advection scheme
real part: phase characteristic
imaginary part (is negative): damping

Splitting error term

Higher order terms

Courant numbers

Euler forward

$$S.E.T. = N k_{c_s} c_s \Re(k_U) U$$

Wicker/Skamarock

$$S.E.T. = 0.625 N k_{c_s} c_s \Re(k_U) \Im(k_U) U^2$$

Gassmann

$$S.E.T. = 0.125 N k_{c_s} c_s \Re(k_U) \Im(k_U) U^2$$

Numerical analysis of the sound advection system

Stability diagrams for an 8 Δx wave

Euler forward | Wicker/Skamarock | Gassmann

Forward moving mode

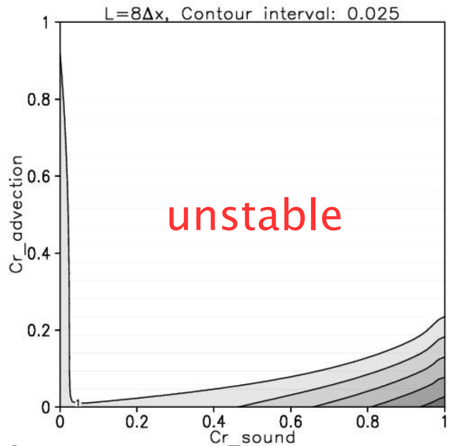

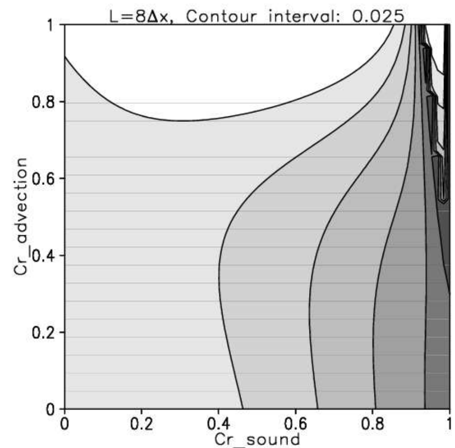

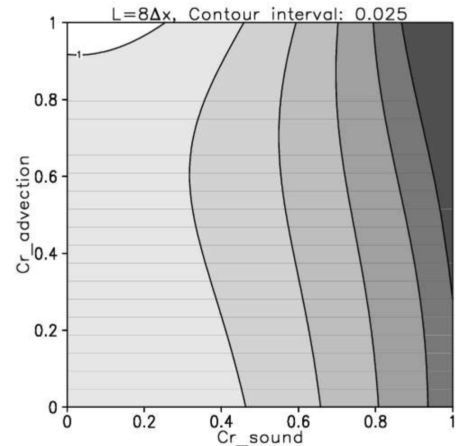

with divergence damping

Backward moving mode

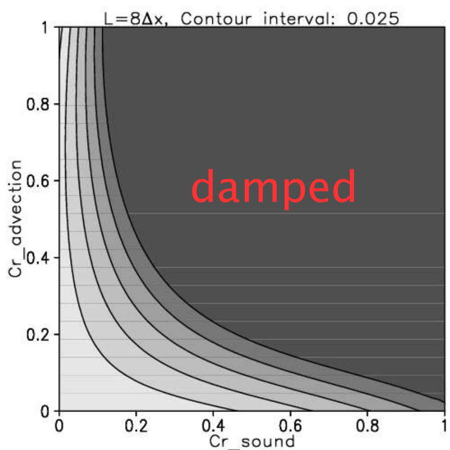

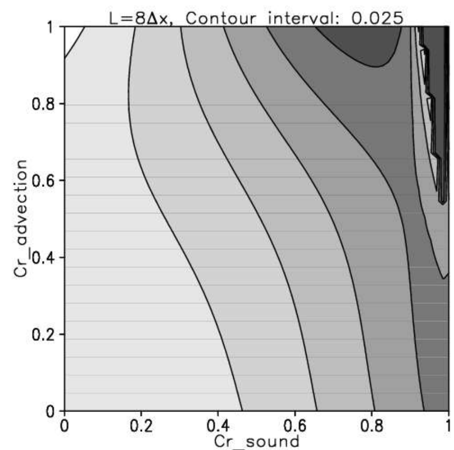

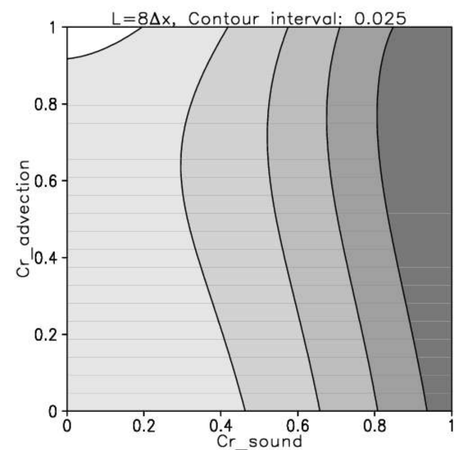

Splitting scheme analysis with the linear nonhydrostatic compressible system

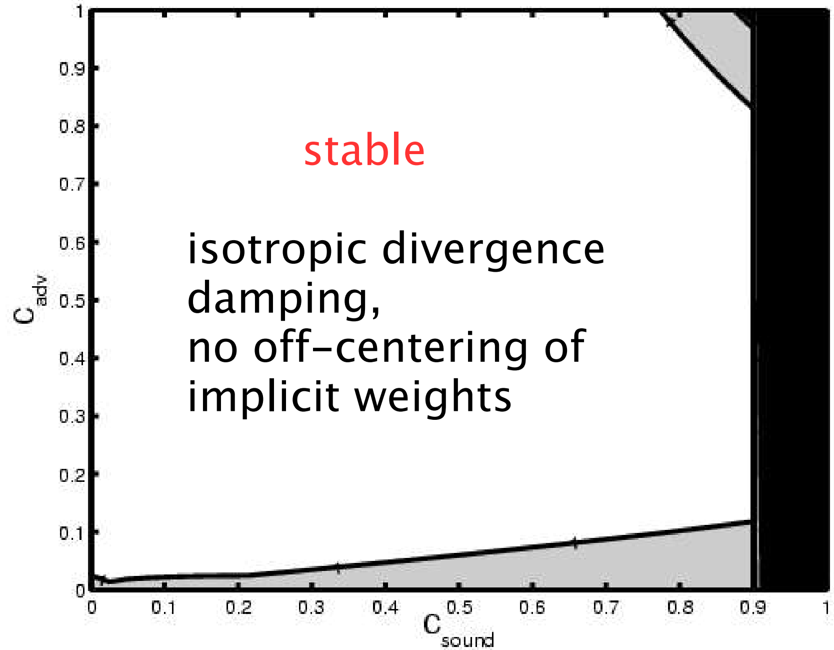

Stability diagrams of the Gassmann scheme

no divergence damping,
no offcentering of implicit weights

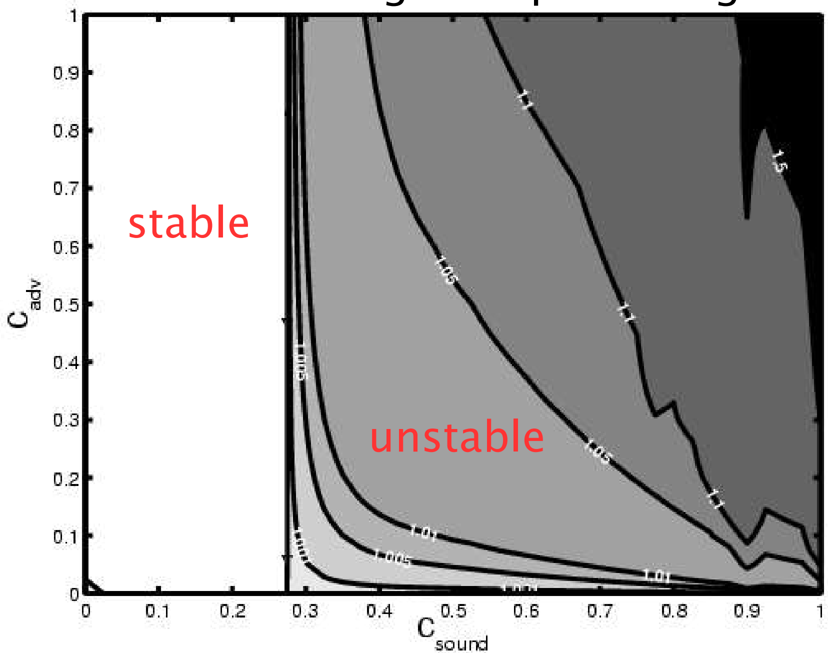

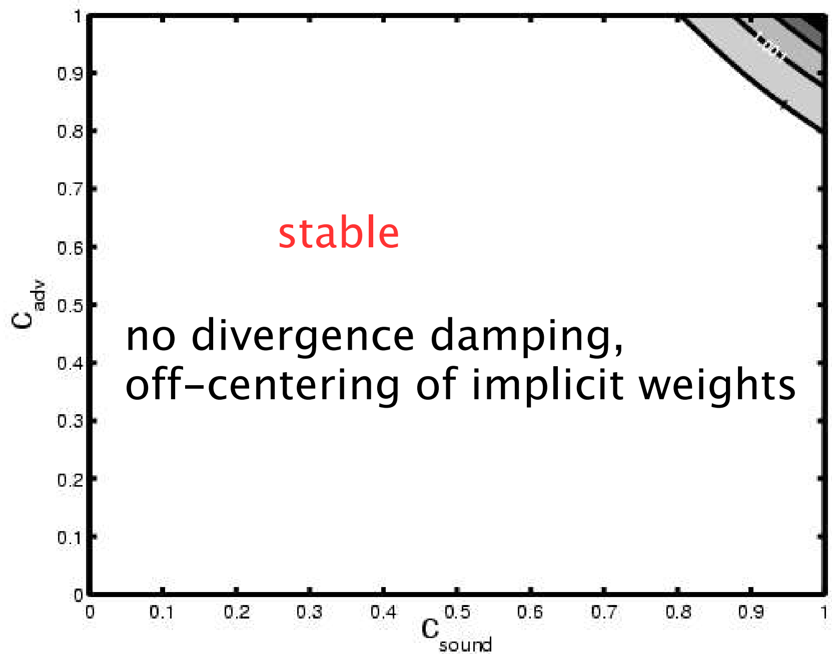

Splitting schemes – Conclusions

•Though the advection scheme and the fast-waves scheme may be stable for themselves, the combination in the splitting scheme is not automatically stable!

•The splitting error term is a multiplicative combination of both parts and contains the significant propagation information, and so never vanishes: it may only be reduced.

•An additional damping mechanism (hidden in H.O.T.) is essential.

•The propagation of waves in different directions (modes) is either amplified or damped.

•The Gassmann-scheme is shown to be the best compromise among the candidates presented.

•The stability analysis of the splitting scheme for the complete nonhydrostatic compressible equations yields satisfactory results.

Other variants of splitting schemes – Strang splitting

Strang

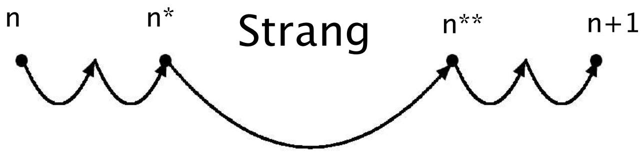

Klemp/Wilhelmson

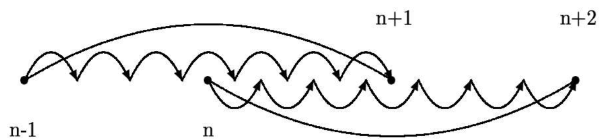

A gravity wave generator is situated in the center of the domain, the ambient horizontal wind increases with height from 5 to 15m/s.

Since the operators for each fractional step do not commute, the stability of each individual operator no longer guarantees the stability of the overall scheme.

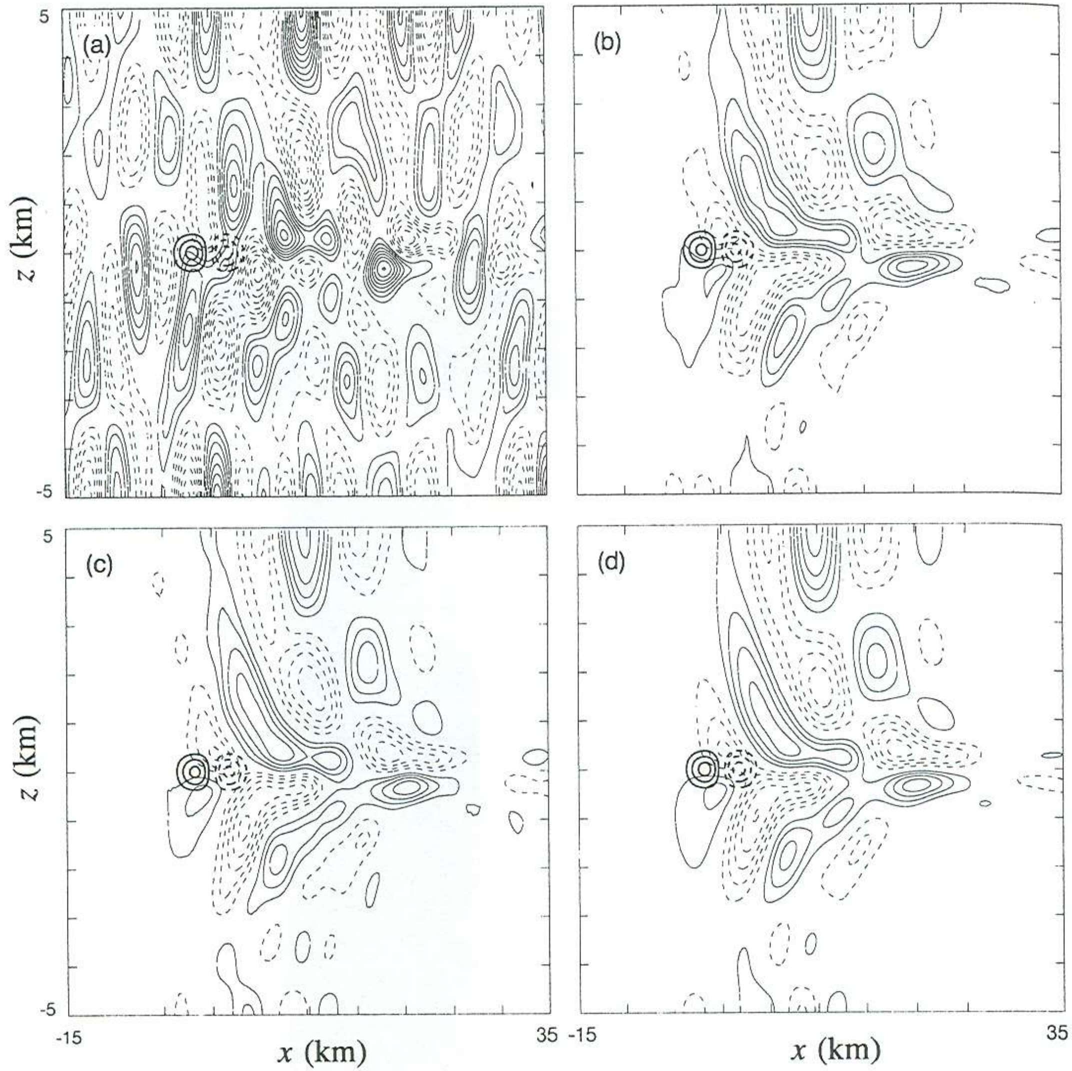

FIGURE 7.3. Contours of P at intervals of 0.25 m^2s^{-2} and Ψ at intervals of 0.1 s^{-1} at t = 3000 s for the case with vertical shear in the mean wind and (a) $\Delta t = 12.5$ s, $M = 20$, (b) $\Delta t = 6.25$ s, $M = 20$, (c) $\Delta t = 6.25$ s, $M = 10$, (d) the solution is computed using the partial splitting method described in the next section with $\Delta t = 12.5$ s, $M = 20$. No zero contours are plotted. Major tick marks appear every 20 grid intervals.

From Durran (1999)

Other variants of splitting schemes - Runge Kutta type advection

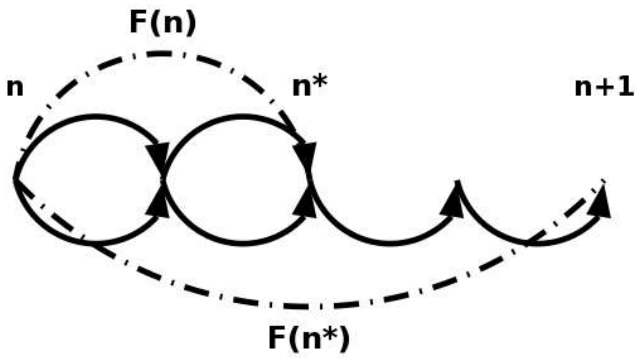

Runge-Kutta-2nd order in time

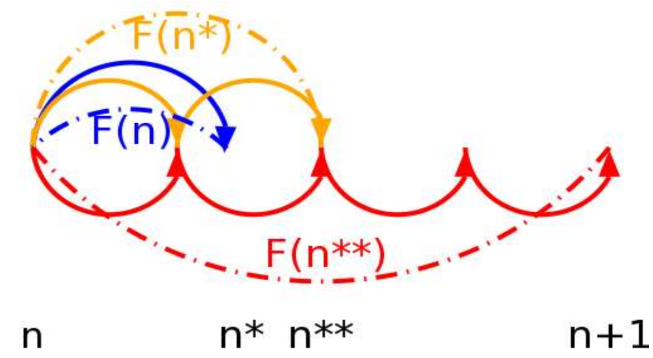

Runge-Kutta-3rd order in time

TABLE 1. Maximum stable Courant number for one-dimensional linear advection. Here, U indicates the scheme is unstable.

	Spatial order			
Time scheme	3rd	4th	5th	6th
Leapfrog	U	0.72	U	0.62
RK2	0.88	U	0.30	U
RK3	1.61	1.26	1.42	1.08

But the Gassmann scheme is independent of the actual advection scheme and may be combined with RK3.

Larger Courant numbers for RK3 and higher accuracy in space!

From Wicker and Skamarock (2002), cf. also WRF-Documentation

Applications – Consequences for the LM

The nonhydrostatic compressible LM (Lokal-Modell) is the operational regional forecast model of the COSMO group. Its dynamical core reads:

$$\frac{\partial u}{\partial t} + \frac{1}{\varrho a \cos\varphi}\left(\frac{\partial p'}{\partial \lambda} + \frac{1}{\sqrt{G}}\frac{\partial z}{\partial \lambda}\frac{\partial p'}{\partial \zeta}\right) = s_u \qquad s_u = fv - \frac{1}{a\cos\varphi}\left(u\frac{\partial u}{\partial \lambda} + v\cos\varphi\frac{\partial u}{\partial \varphi}\right) - \dot{\zeta}\frac{\partial u}{\partial \zeta} + \frac{uv}{a}\tan\varphi$$

$$\frac{\partial v}{\partial t} + \frac{1}{\varrho a}\left(\frac{\partial p'}{\partial \varphi} + \frac{1}{\sqrt{G}}\frac{\partial z}{\partial \varphi}\frac{\partial p'}{\partial \zeta}\right) = s_v \qquad s_v = -fu - \frac{1}{a\cos\varphi}\left(u\frac{\partial v}{\partial \lambda} + v\cos\varphi\frac{\partial v}{\partial \varphi}\right) - \dot{\zeta}\frac{\partial v}{\partial \zeta} - \frac{u^2}{a}\tan\varphi$$

$$\frac{\partial w}{\partial t} - \frac{1}{\varrho\sqrt{G}}\frac{\partial p'}{\partial \zeta} + \frac{g}{\varrho T R_d}p' - g\frac{\varrho_0}{\varrho}\left(\frac{T - T_0}{T}\right) = s_w \qquad s_w = -\frac{1}{a\cos\varphi}\left(u\frac{\partial w}{\partial \lambda} + v\cos\varphi\frac{\partial w}{\partial \varphi}\right) - \dot{\zeta}\frac{\partial w}{\partial \zeta}$$

$$\frac{\partial p'}{\partial t}\boxed{- \frac{1}{\sqrt{G}}\frac{\partial p}{\partial \zeta}w} + \frac{c_{pd}}{c_{vd}}p\left(D_h - \frac{1}{\sqrt{G}}\frac{\partial w}{\partial \zeta}\right) = s_{p'} \qquad s_{p'} = -\frac{1}{a\cos\varphi}\left(u\frac{\partial p'}{\partial \lambda} + v\cos\varphi\frac{\partial p'}{\partial \varphi}\right)\boxed{- \dot{\xi}\frac{\partial p'}{\partial \zeta}}$$

$$\frac{\partial T}{\partial t}\boxed{- \frac{1}{\sqrt{G}}\frac{\partial T}{\partial \zeta}w} + \frac{p}{c_{vd}\varrho}\left(D_h - \frac{1}{\sqrt{G}}\frac{\partial w}{\partial \zeta}\right) = s_T \qquad s_T = -\frac{1}{a\cos\varphi}\left(u\frac{\partial T}{\partial \lambda} + v\cos\varphi\frac{\partial T}{\partial \varphi}\right)\boxed{- \dot{\xi}\frac{\partial T}{\partial \zeta}}$$

$$\dot{\zeta} = \dot{\xi} - \frac{1}{\sqrt{G}}w$$

usual contravariant vertical velocity

$$\boxed{\dot{\xi} = \frac{1}{\sqrt{G}}\left(\frac{u}{a\cos\varphi}\frac{\partial z}{\partial \lambda} + \frac{v}{a}\frac{\partial z}{\partial \varphi}\right)}$$

vertical velocity related to the terrain following coordinates

Applications – Consequences for the LM

Schaer test case with Gassmann-splitting

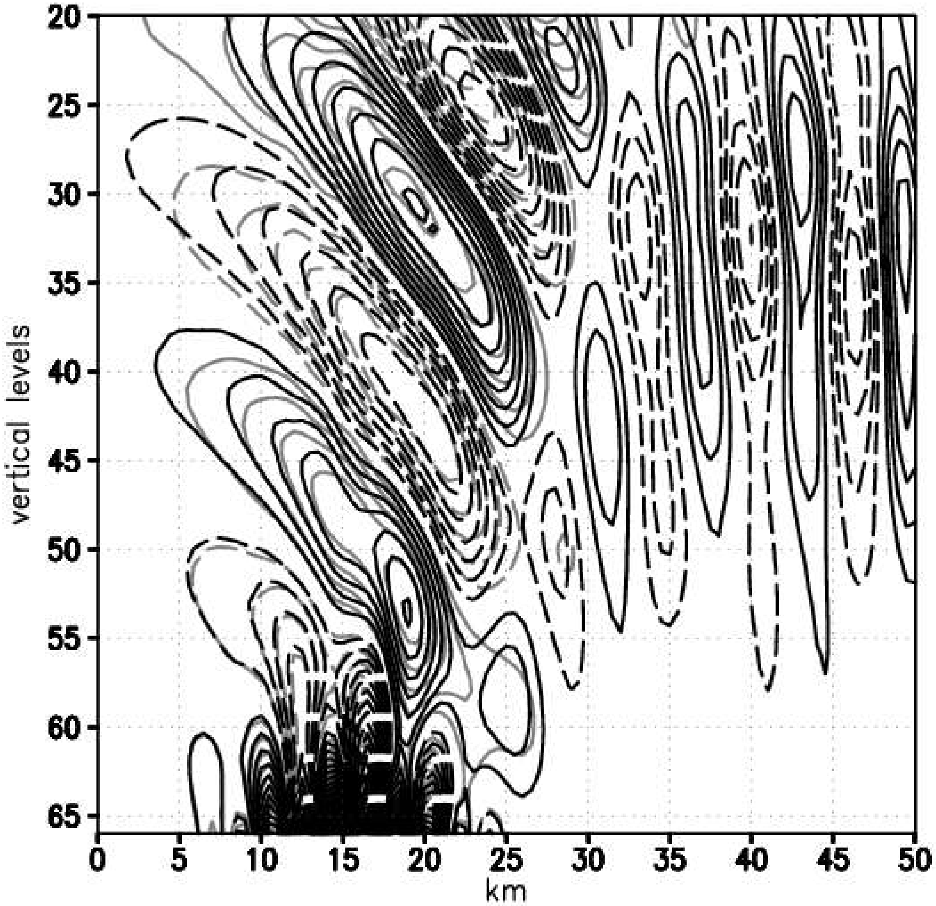

vertical advection of T and p' in slow modes

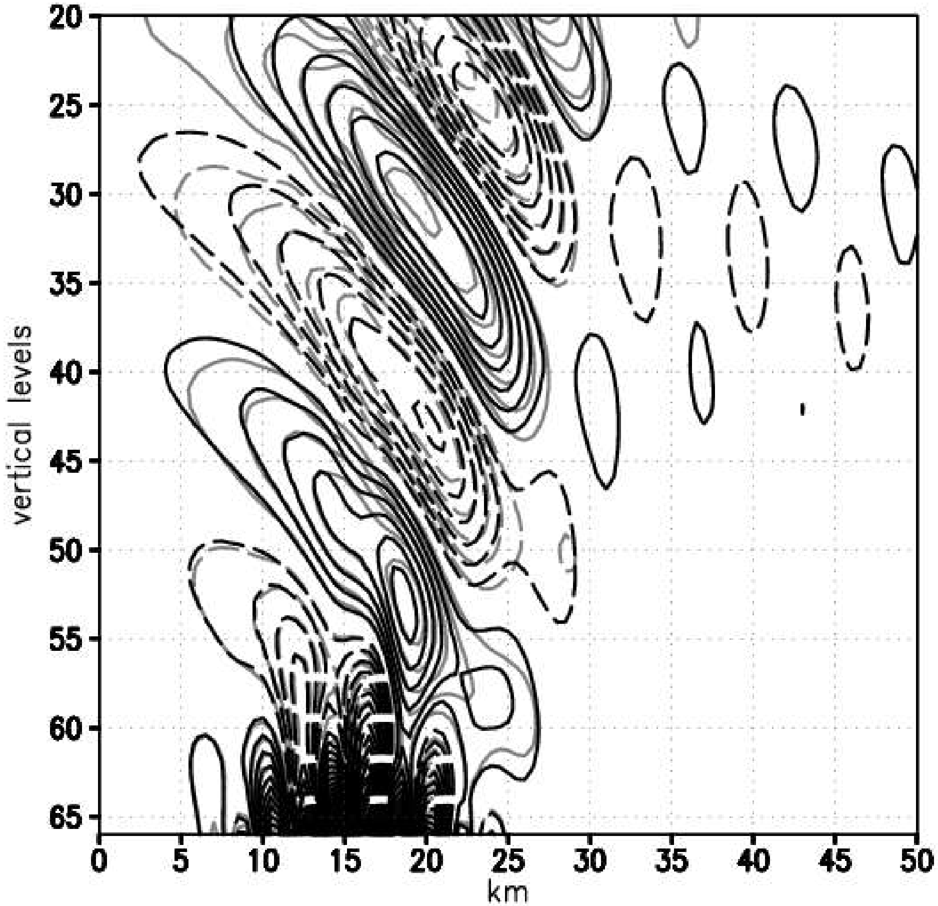

vertical advection of T and p' in fast modes

Applications – Consequences for the LM

Radiative upper boundary condition – RUBC

With the new fast waves algorithm all information for gravity waves is included in the fast-waves part. That is the prerequisite for applying the radiative upper boundary condition directly in the vertical implicit solver of the fast-waves.

$$\hat{w} = \frac{K}{\overline{\overline{N\varrho}}}\hat{p}'$$

relation for hydrostatic gravity waves at the model top

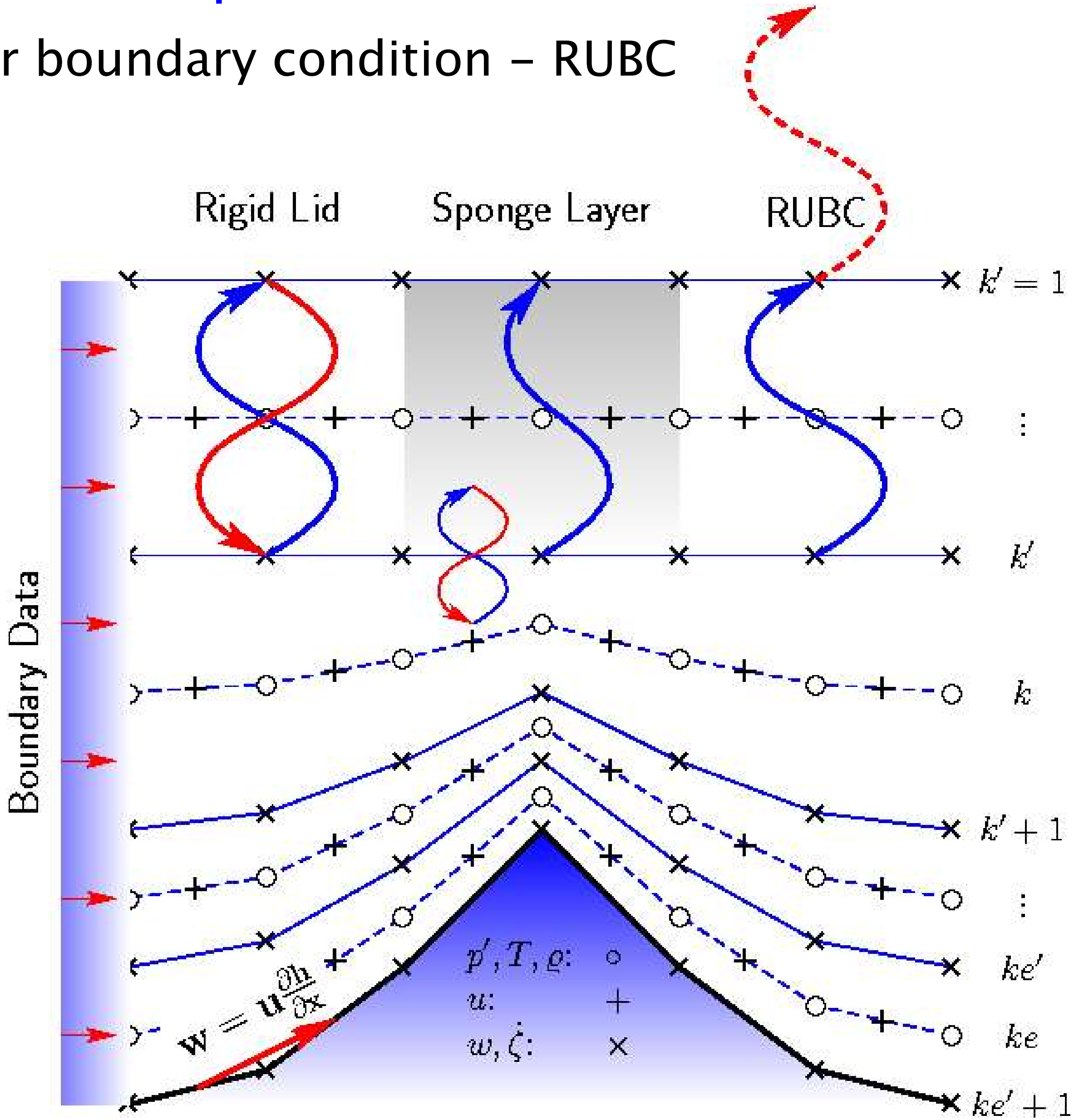

Applications – Consequences for the LM

Schaer
test case
with RUBC

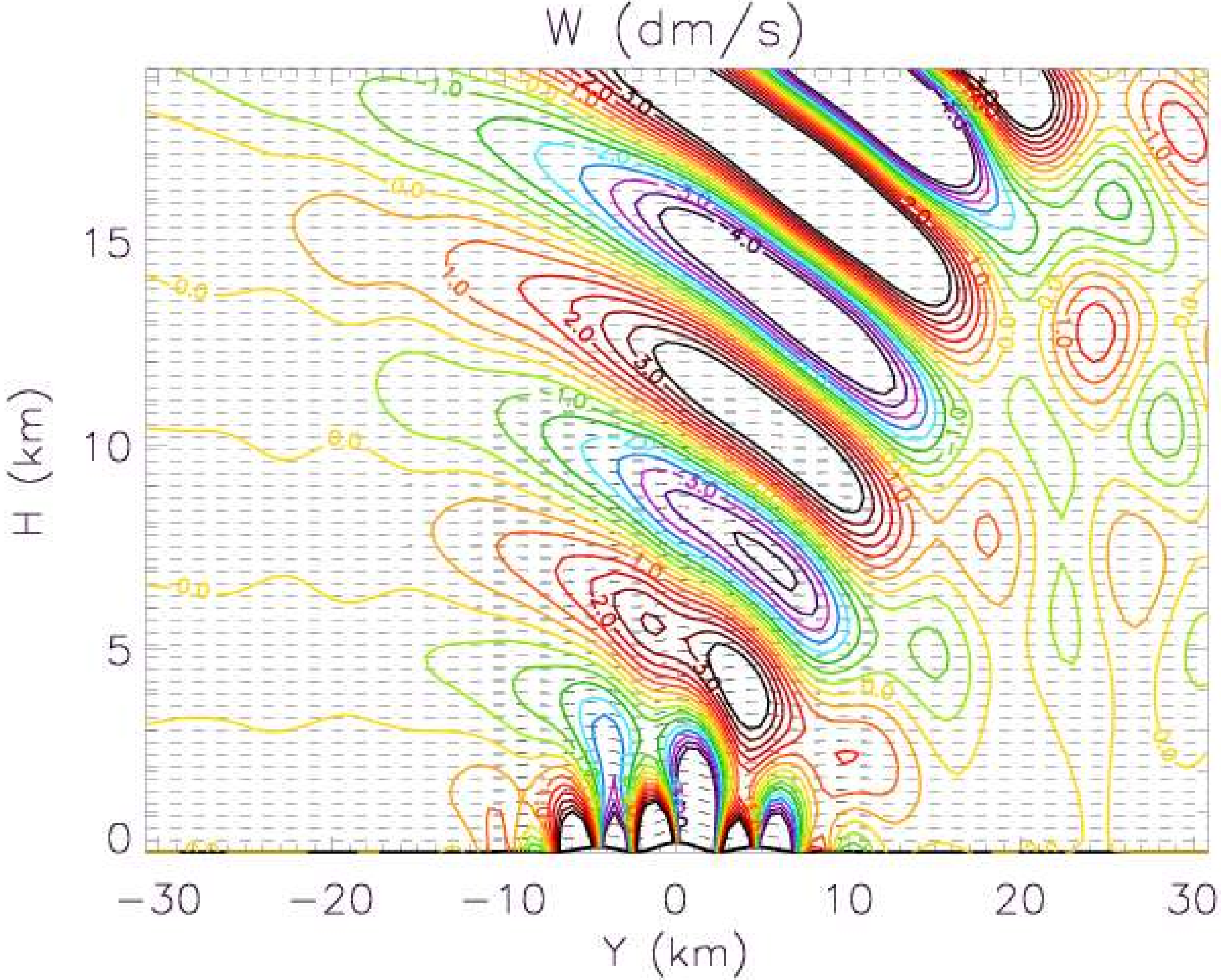

Applications – Consequences for the LM

Schaer test case with sponge upper boundary condition

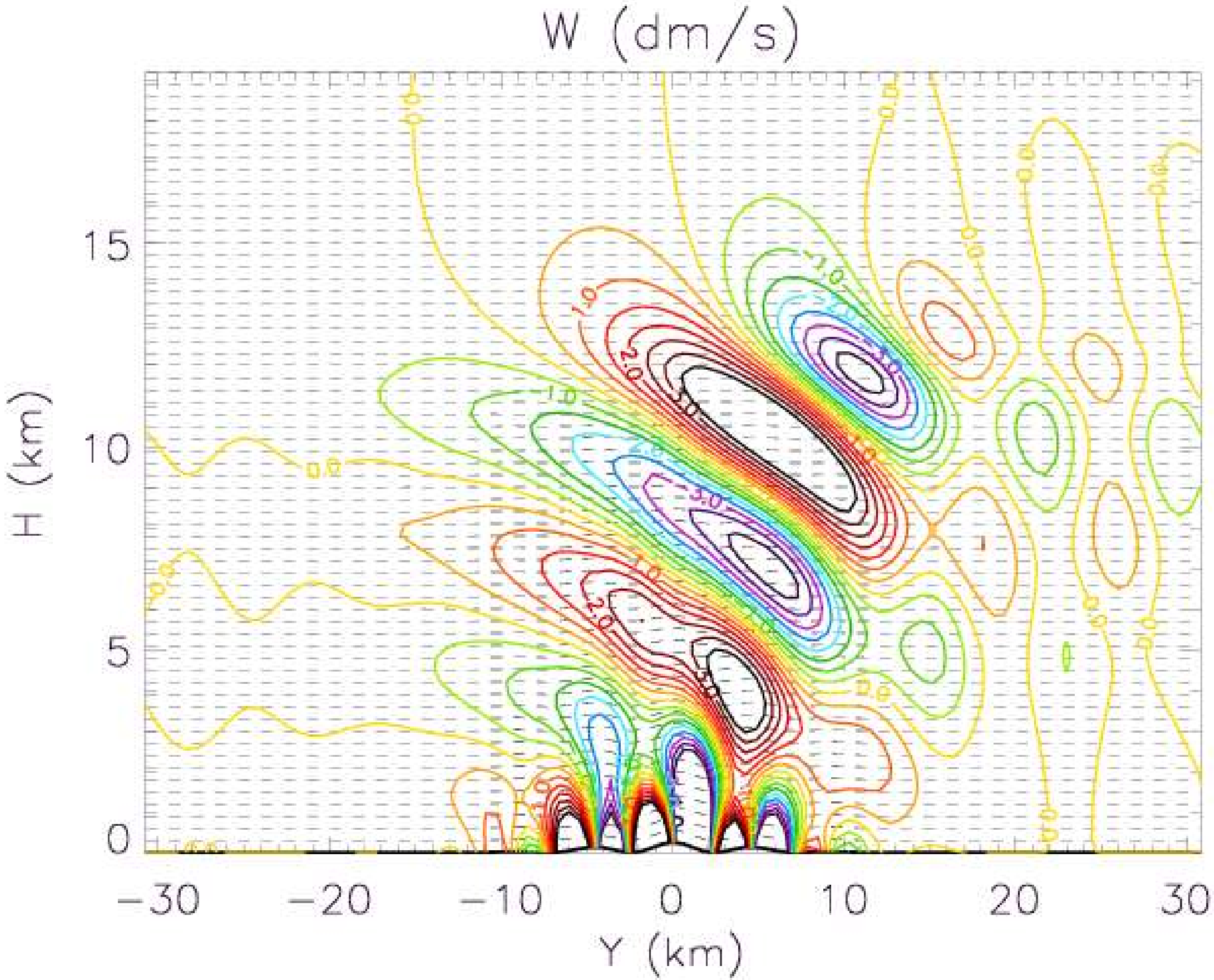

Applications – Consequences for the LM

Schaer test case with sponge upper boundary condition

old LM dynamics

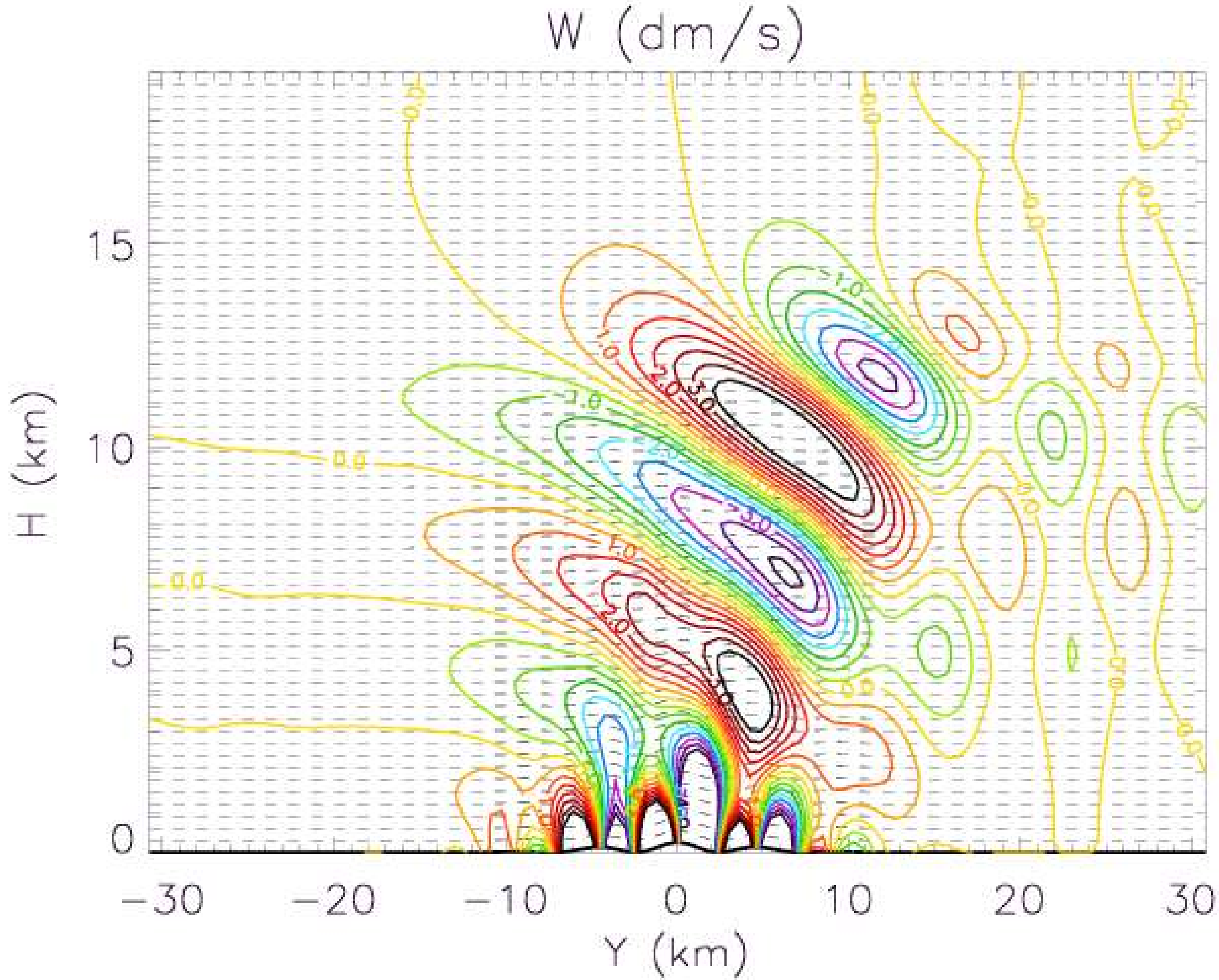

Applications – Consequences for the LM

with
Radiative
Upper
Boundary
Condition

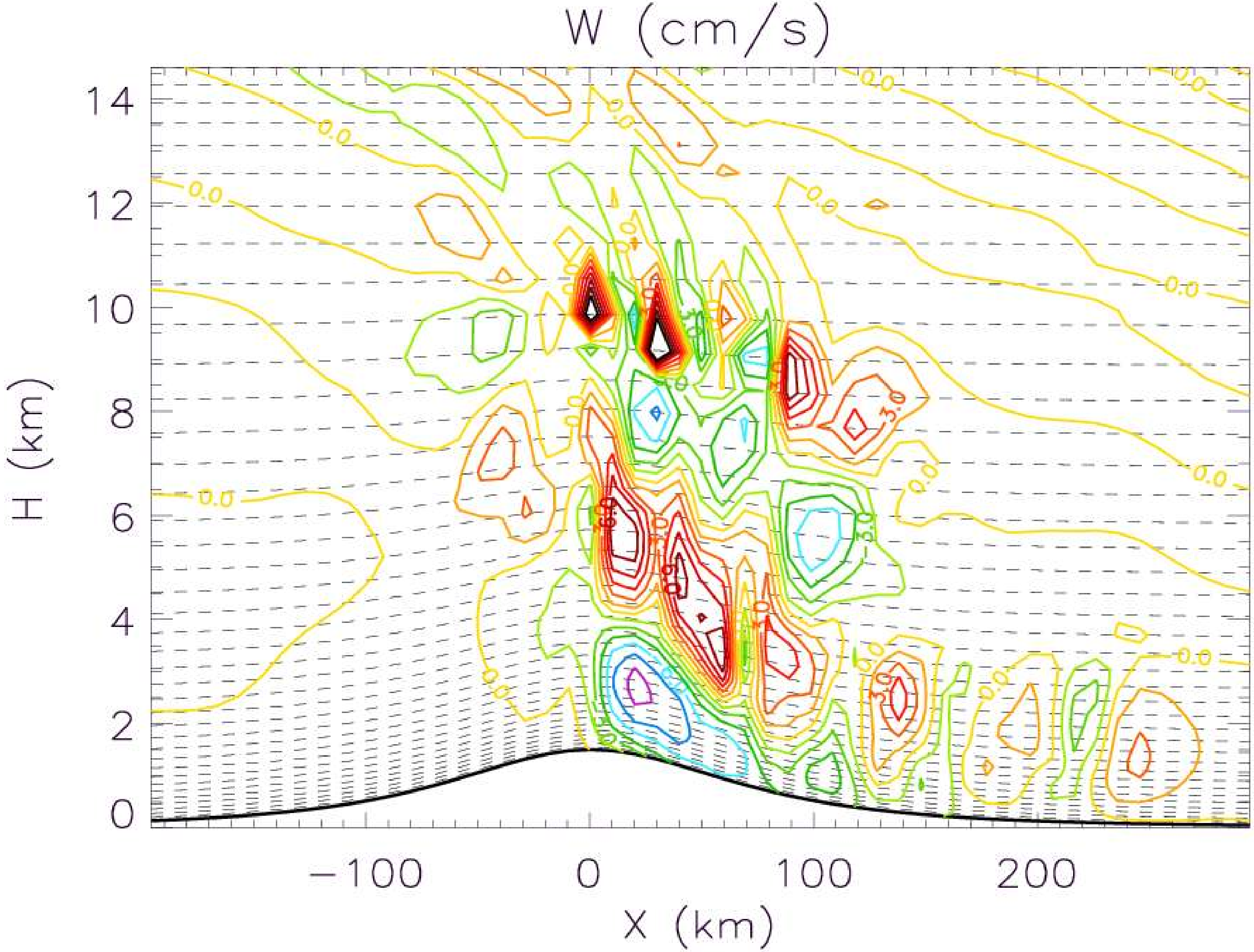

Nonlinear flow past a high mountain, dx=7km, tropopause at 10km, realistic vertical levels

Applications - Consequences for the LM

Old LM dynamics.
Without and with dynamic lower boundary condition in the horizontal momentum equations.

Resting atmosphere over a high mountain

New LM dynamics.
With sponge layer and with RUBC.

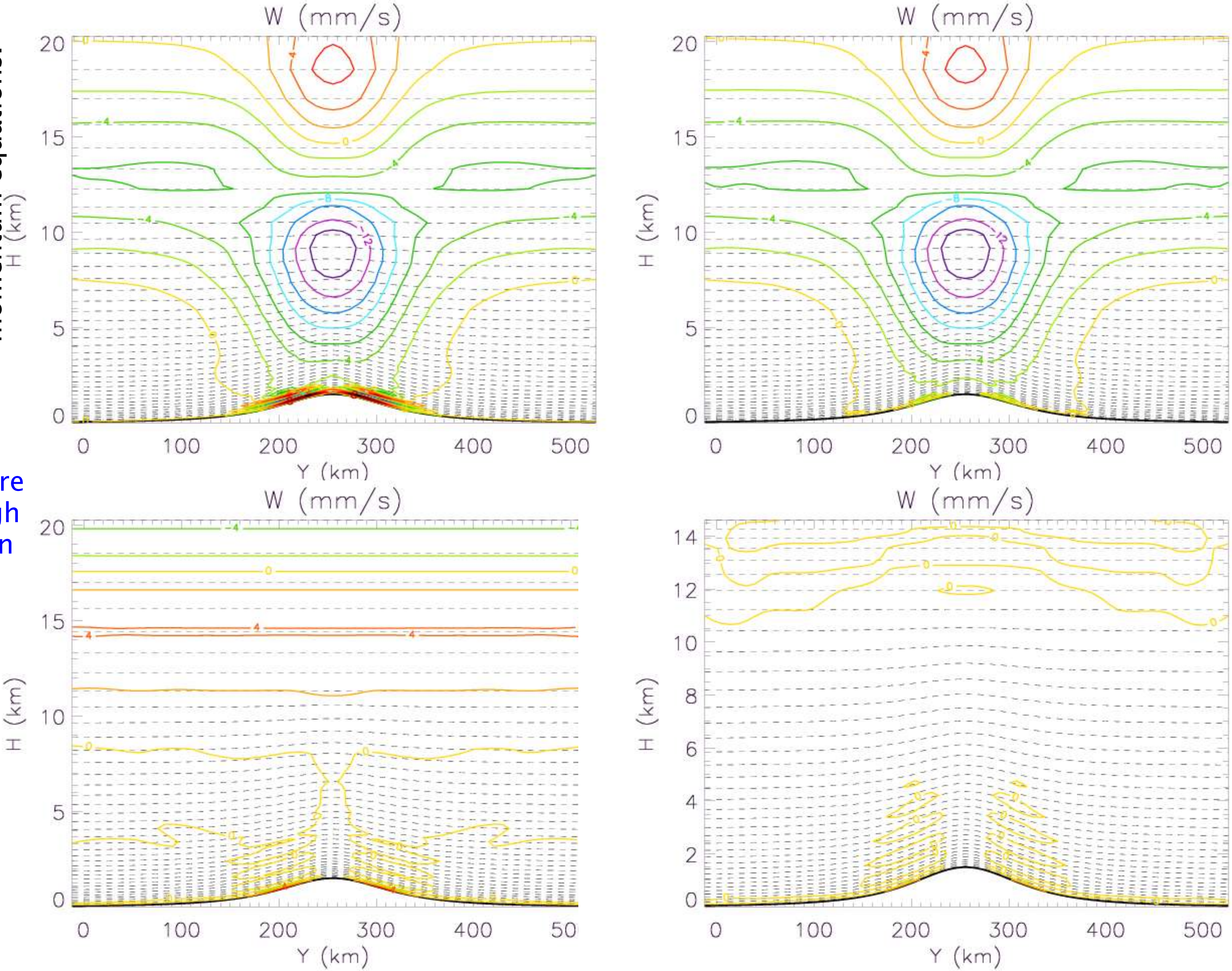

Applications – Consequences for the LMK (LM-short range forecast)

TVD-Runge-Kutta scheme

$$
\begin{aligned}
\psi_i^* &= \psi_i^n + \Delta t F(\psi^n)_i \\
\psi_i^{**} &= \frac{3}{4}\psi_i^n + \frac{1}{4}\psi_i^* + \frac{1}{4}\Delta t F(\psi^*)_i \\
\psi_i^{n+1} &= \frac{1}{3}\psi_i^n + \frac{2}{3}\psi_i^{**} + \frac{2}{3}\Delta t F(\psi^{**})_i
\end{aligned}
$$

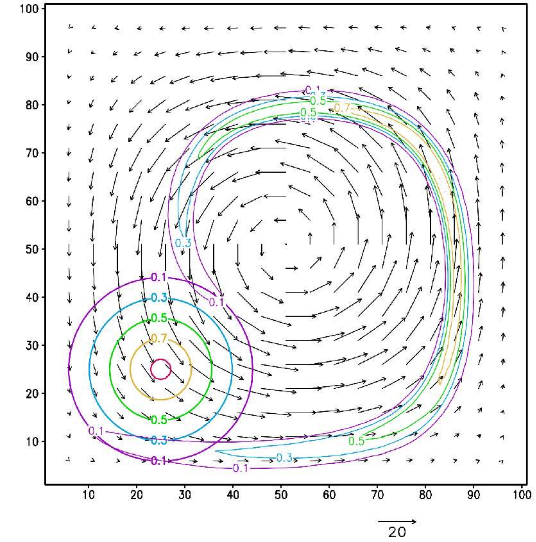

Solid Body Rotation of a tracer cone with an initial maximum of 1, 400 time steps for one turn

RK-3rd / CD-4th	RK-3rd / CD-4th + HD	TVD-RK-3rd / CD-4th
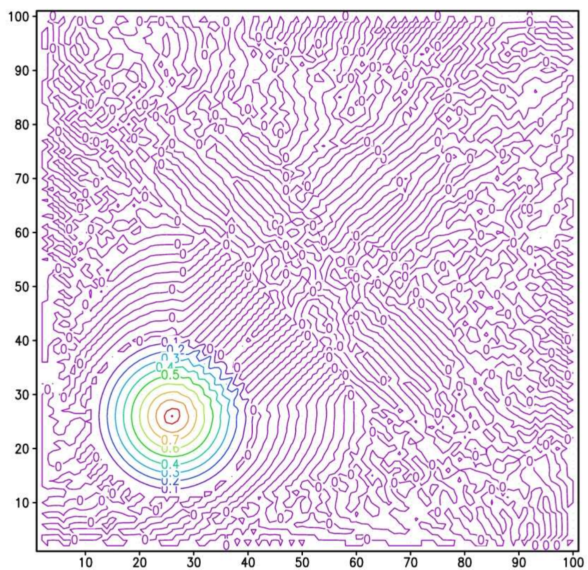	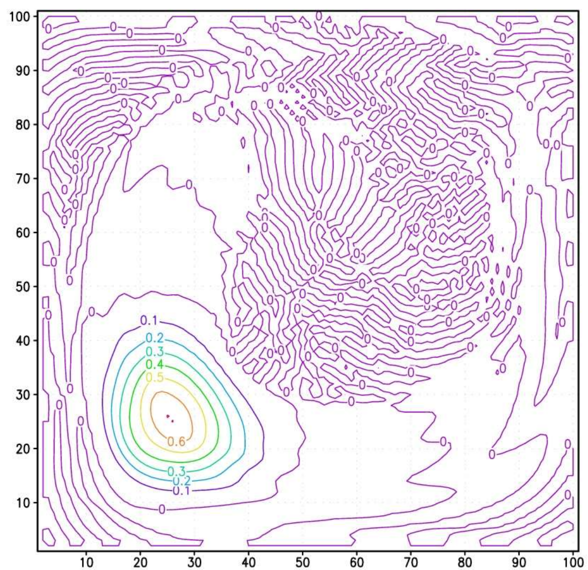	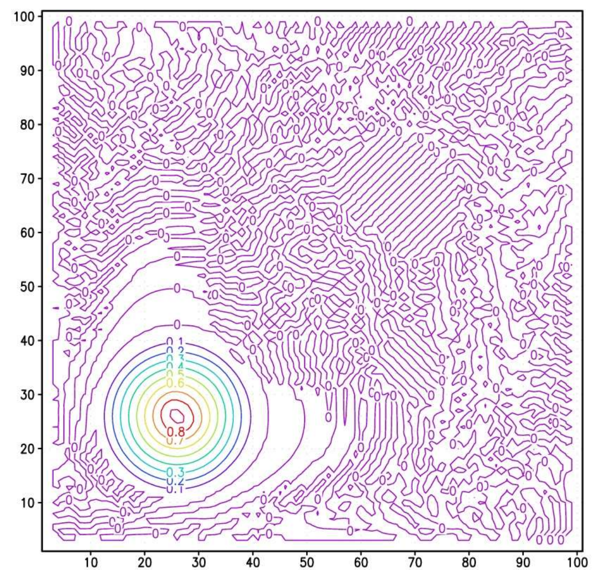
670 time steps	550 time steps	450 time steps

Figures from Jochen Foerstner, DWD

Applications – Consequences for the LMK (LM-short range forecast)

TVD-Runge-Kutta scheme now applied within the framework of the Wicker/Skamarock-splitting

advection of a tracer without fast-waves TVD-RK3/5th upwind

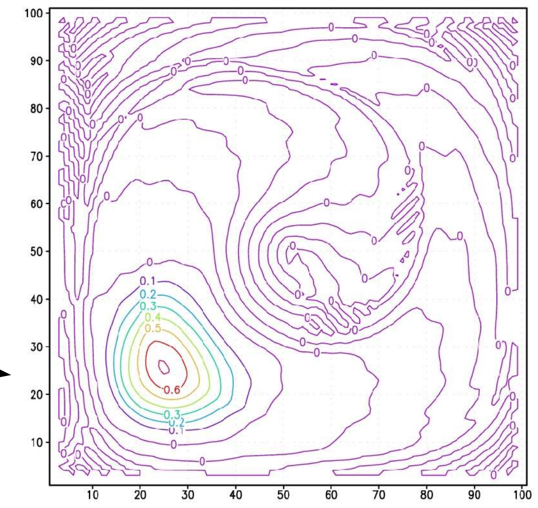

TVD-RK3/4thCD

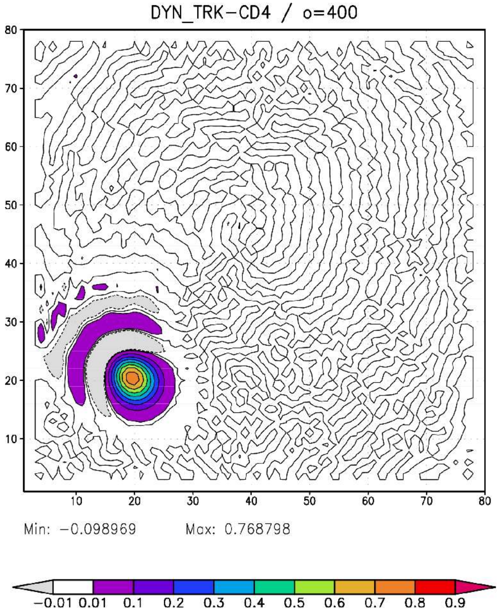

TVD-RK3/4thCD +horizontal diffusion

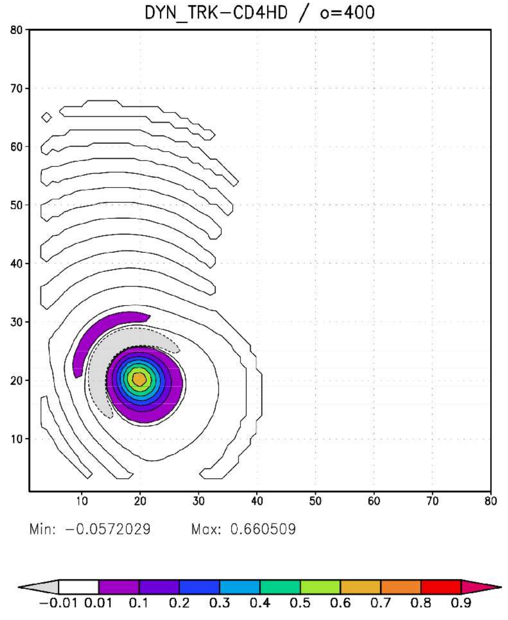

TVD-RK3/5thupwind

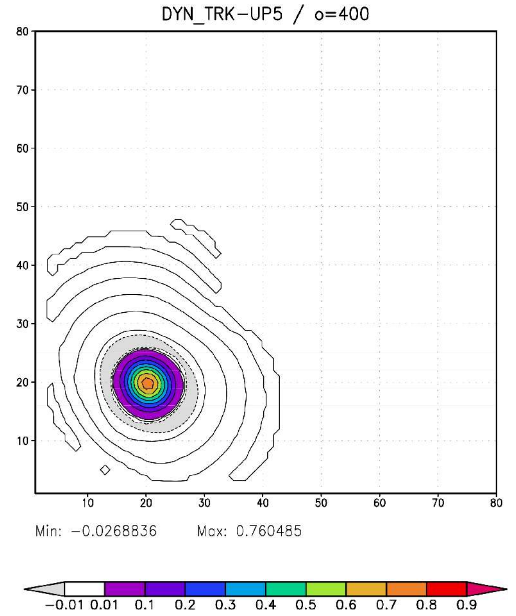

Figures from Jochen Foerstner, DWD

Applications – Conservative split-explicit WRF version

WRF – Weather Research and Forecasting modeling system

collaboration amongst NCAR, NOAA, FSL, AFWA, NRL, CAPS, FAA in the U.S.A.

Flux quantities

$$\mathbf{V} = \rho\mathbf{v} = (U, V, W), \qquad \Theta = \rho\theta,$$

Flux form equations

$$\partial_t U + \boldsymbol{\nabla}\cdot(\mathbf{v}U) + \partial_x p' = F_U$$

$$\partial_t V + \boldsymbol{\nabla}\cdot(\mathbf{v}V) + \partial_y p' = F_V$$

$$\partial_t W + \boldsymbol{\nabla}\cdot(\mathbf{v}W) + \partial_z p' + g\rho' = F_W$$

$$\partial_t \Theta + \boldsymbol{\nabla}\cdot(\mathbf{v}\Theta) = F_\Theta$$

$$\partial_t \rho' + \boldsymbol{\nabla}\cdot\mathbf{V} = 0.$$

How to linearize these equations for splitting off the fast-waves part?

$$\mathbf{V}'' = \mathbf{V} - \mathbf{V}^t = (U - U^t, V - V^t, W - W^t),\ \Theta'' = \Theta - \Theta^t, \text{ and } \rho'' = \rho - \rho^t$$

This corresponds to a linearization around the present time step t.

slow modes

$$\partial_t U'' + \gamma R \pi^t \partial_x \Theta'' = F_U{}^t - \partial_x p'^t - \boldsymbol{\nabla}\cdot(\mathbf{v}^t U^t)$$

$$\partial_t V'' + \gamma R \pi^t \partial_y \Theta'' = F_V{}^t - \partial_y p'^t - \boldsymbol{\nabla}\cdot(\mathbf{v}^t V^t)$$

$$\partial_t W'' + \gamma R \pi^t \partial_z \Theta'' - g\bar{\rho}\frac{R}{c_v}\frac{\pi^t}{\bar{\pi}}\frac{\Theta''}{\bar{\Theta}} + g\rho'' = F_W{}^t - \partial_z p'^t - g\rho'^t - \boldsymbol{\nabla}\cdot(\mathbf{v}^t W^t)$$

$$\partial_t \Theta'' + \boldsymbol{\nabla}\cdot(\mathbf{V}''\theta^t) = F_\Theta{}^t - \boldsymbol{\nabla}\cdot(\mathbf{v}^t\Theta^t)$$

$$\partial_t \rho'' + \boldsymbol{\nabla}\cdot\mathbf{V}'' = -\boldsymbol{\nabla}\cdot\mathbf{V}^t$$

fast modes

From Klemp et al., 2000, cf. also Skamarock et al. 2005

Summary on split-explicit methods

- The split explicit method is an efficient and accurate method for integrating the unfiltered hydro-thermodynamic equations.
- The method is easily implemented also on parallel platforms.
- Numerical stability is the crucial point in designing split-explicit schemes.
- Another problem is the proper mode splitting.
- The combination with different advection schemes is possible.
- Split-explicit time integration is even applicable to the flux-form equations.
- Features like the radiative upper boundary condition are easily included in the complete algorithm.